

NASA TM- 88221

NASA Technical Memorandum 88221

NASA-TM-88221 19860022351

Numerical Simulation of Boundary Layers: Part 2. Ribbon-Induced Transition in Blasius Flow

Philippe R. Spalart and Kyung-Soo Yang

February 1986

LIBRARY COPY

MAR 4 1986

LANGLEY RESEARCH CENTER
LIBRARY, NASA
HAMPTON, VIRGINIA

NASA
National Aeronautics and
Space Administration



NF00938

Numerical Simulation of Boundary Layers: Part 2. Ribbon-Induced Transition in Blasius Flow

Philippe R. Spalart, Ames Research Center, Moffett Field, California
Kyung-Soo Yang, Stanford University, Stanford, California

February 1986

NASA

National Aeronautics and
Space Administration

Ames Research Center

Moffett Field, California 94035

186-31823 #

Numerical simulation of boundary layers

Part 2. Ribbon-induced transition in Blasius flow

By PHILIPPE R. SPALART and KYUNG-SOO YANG

NASA Ames Research Center, Moffett Field, California 94035

and

Stanford University, Stanford, California 94305

The early three-dimensional stages of transition in Blasius boundary layers are studied by numerical solution of the Navier-Stokes equations. A finite-amplitude two-dimensional wave and random low-amplitude three-dimensional disturbances are introduced. Rapid amplification of the three-dimensional components is observed and leads to transition. For intermediate amplitudes of the two-dimensional wave the breakdown is of subharmonic type, and the dominant spanwise wave number increases with the amplitude. For high amplitudes the energy of the fundamental mode is comparable to the energy of the subharmonic mode, but never dominates it; the breakdown is of mixed type. Visualizations, energy histories, and spectra are presented. The sensitivity of the results to various physical and numerical parameters is studied. The agreement with experimental and theoretical results is discussed.

1. Introduction

Our ability to understand, predict, and control the transition of fluid flows from laminar to turbulent states is far from satisfactory, in spite of decades of effort. Transition is very sensitive both to the exact shape of the basic laminar flow and to the detailed characteristics (amplitude, spectrum, etc.) of the disturbances, whether they are associated with the stream or with the surface. Natural transition is very intermittent and thus is difficult to measure. The control of transition would allow significant improvements in many applications; for instance, reduced skin-friction drag or higher lift coefficients for wings, or enhanced mixing for combustion and chemical reactions.

Several stages can be distinguished as one observes the transition of a boundary layer starting from upstream. At first the disturbances, within the basic laminar flow, are small enough to be described by the linear Orr-Sommerfeld equation (Schlichting 1979). The "linear" behavior of single two-dimensional and oblique Tollmien-Schlichting (TS) waves is well understood, but in practice numerous waves compete and grow simultaneously. The slow thickening of the boundary layer adds to the complexity of the situation. In any case, linearized theory is insufficient to predict transition, because it fails to predict the large growth rates that are observed. The linear stage is followed by an "early nonlinear" stage during which nonlinear effects become significant, but the disturbances are still rather weak and the flow is still smooth. The nonlinear effects are revealed by much larger

growth rates of some of the disturbances, which are invariably three-dimensional. Two-dimensional nonlinear effects, such as the saturation of a TS wave, are benign and are unable to induce transition, probably because of the absence of vortex stretching. Finally, there is a strongly nonlinear stage which leads to the fully turbulent boundary layer, with intense fluctuations and fine scales of motion.

The early nonlinear stage has been the subject of recent experimental, theoretical, and numerical work (Kachanov & Levchenko 1984, Saric *et al.* 1984, Craik 1971, Herbert 1984, Herbert 1985, Wray & Hussaini 1984, Spalart 1984). Because the flow is still smooth, this stage is easier to study than the strongly nonlinear stage. It is also more important in terms of transition control, because full transition is inevitable once the strongly nonlinear stage has been reached. Thus, efforts to prevent transition (for instance pressure gradients, suction, or even active control of the waves) must be applied during the early stage, at the latest.

In most experimental studies a two-dimensional wave is introduced by means of a vibrating ribbon, so that it dominates the other unstable waves during the linear stage. This makes the experiment more reproducible. The theoretical and numerical studies, excepting Craik's work (1971), also involve a dominant two-dimensional wave. This procedure should be considered as a first step toward the study of "natural" transition. Natural transition generally involves wave packets rather than single waves.

In the experiments of Klebanoff *et al.* (1962) and Kovasznay *et al.* (1962), with a vibrating ribbon, the first strong three-dimensional structures to appear were quasi-periodic in the streamwise direction, with the same period as the fundamental wave. The structures were also quasi-periodic in the spanwise direction, with a period of the same order. These structures contain "A vortices," a result of the deformation of the spanwise vorticity contained in the mean flow and the TS wave. As these structures evolve, and presumably under the effect of vortex stretching, the flow exhibits an increasing number of "spikes" in the velocity field, which are the first signs of turbulence. This phenomenon was accurately simulated, numerically, by Wray & Hussaini (1984). Similar simulations were conducted in the channel by Orszag & Kells (1980).

The significant discovery of the last few years is that the streamwise period of the early three-dimensional structures can also be twice the period of the fundamental wave (Kachanov & Levchenko 1984, Saric *et al.* 1984). This is the "subharmonic" type of breakdown, in which the A vortices are staggered as on a checkerboard. The experiments also indicate that subharmonic breakdown occurs for low and intermediate amplitudes of the two-dimensional wave, while the "fundamental" or "peak-valley" type occurs for higher amplitudes. If the wave amplitude is too low, it fails to cause transition and decays. Craik (1971) and Herbert (1984) have proposed weakly nonlinear theories that can predict an instability of the subharmonic type. Craik's model involves a resonant triad (a two-dimensional wave and two oblique waves), while Herbert's model involves the linear instability of three-dimensional waves in presence of a finite-amplitude two-dimensional wave. Craik's mechanism is thought to dominate at low amplitudes (hence the designation C-type), while Herbert's mechanism describes intermediate-amplitude situations better (hence the designation H-type). Another version of Herbert's theory also predicts the fundamental or K-type breakdown (Herbert 1985).

The discovery of subharmonic breakdown presented a new challenge for numerical simulations. Preliminary results of the present study, presented by Spalart (1984), indicated that the two types of breakdown were indeed predicted, depending on the amplitude. The quantitative agreement with experiments was fair. More complete and accurate results are presented here. This paper is Part 2 of an article on direct numerical simulations of

boundary layers. Part 1 introduced the method, and Part 3 describes simulations of fully turbulent boundary layers.

Experiments, small-disturbance theories, and numerical simulations all complement each other in the study of transition. Compared with weakly nonlinear models a direct numerical study, while more expensive, has several advantages. The simulation is fully nonlinear and the “shape assumption” invoked by Herbert (1984) is not necessary. The spectrum is much larger, although it is still bounded and discrete. Random disturbances can be introduced and monitored concurrently in order to compare several possible instability mechanisms. Ensemble averages can be generated. The thickness of the mean flow and the amplitude of the primary disturbance evolve, as they do in the real flow, which has an impact on the secondary instability (a quasi-steady assumption is not made). Visualizations of the flow can be compared almost directly with experimental visualizations. The extension to more complex cases (pressure gradient, suction, crossflow, etc.) is straightforward. On the other hand, with the present method the mean flow is still treated as parallel and the fluctuations as spatially periodic, with transition occurring in time instead of space. Wray & Hussaini (1984) also used a parallel assumption and periodic conditions, mainly for reasons of computational cost. When the flow transitions the range of length and time scales widens rapidly, making an accurate numerical solution increasingly costly. The implications of these periodic assumptions will be discussed.

Besides the boundary conditions, the major choice to be made in a simulation of transition is the choice of the initial disturbances. In their numerical studies, Wray & Hussaini (1984, in the boundary layer) and Orszag & Kells (1980, in the channel) used a single pair of oblique waves as the initial three-dimensional disturbances. Their spanwise wave number was indicated by experimental results. In the present study white noise was used as the three-dimensional disturbance in an effort to remove any bias. This required the use of a much larger period in the spanwise direction to provide a fine enough approximation of the continuous spectrum of the real flow. This large value of the period resulted in a fairly coarse numerical grid and prevented the extension of the simulations deep into the nonlinear stage. However, the present simulations can predict the dominant spanwise wave number instead of assuming its value, and the narrow- or broad-band character of the instability. In some experiments there is evidence that the dominant spanwise wave number is dictated by nonuniformities in the mean flow or in the two-dimensional wave (this was intentional in the work of Klebanoff *et al.*). However, in practical situations the disturbances (surface waviness, free-stream noise, etc.) are more likely to have a random character.

2. Formulation

The approach is to solve the full, time-dependent Navier-Stokes equations in the half-space over a plane wall. The initial condition is a Blasius boundary layer disturbed by a finite-amplitude, two-dimensional TS wave and low-amplitude, three-dimensional random noise. This corresponds to the conditions of an experiment, in which the TS wave would be generated by a vibrating ribbon. It remains to choose proper boundary conditions; that is, to find a good compromise between the desire to conduct a thorough and unbiased simulation of the physics and the desire to obtain an accurate solution at a reasonable cost.

In the experiments the disturbance introduced by the vibrating ribbon is periodic in time and quasi-periodic in the x (streamwise) direction, in the sense that its amplitude varies very little over one wave length. In addition, at the early nonlinear stage, the experiments reveal spatial structures (Λ vortices) that are quasi-periodic both in the x and in the z (spanwise) direction. The wave lengths in the two directions are of the same order.

These observations suggest that periodic conditions in x and in z , with adequate values for the periods, should allow a valuable numerical simulation of the phenomena. Transition will occur in time instead of space, and only one or a few Λ vortices will be contained in the numerical domain. Periodic conditions are mathematically convenient and allow a dramatic reduction in the size of the domain of integration, compared with a simulation that would represent the whole spatially developing boundary layer at once. On the other hand, they will result in a significantly different mean velocity profile unless a correction is made.

With periodic conditions in x , the mean flow is independent of x and parallel. The mean velocity component U is a function of the normal coordinate y and the time t , and satisfies

$$\frac{\partial U}{\partial t} - \frac{\partial \tau}{\partial y} = \nu \frac{\partial^2 U}{\partial y^2}. \quad (1)$$

The density is set to 1 and omitted, ν is the kinematic viscosity and τ is the Reynolds stress. During the linear stage τ is negligible and (1) reduces to Stokes' first problem ($U_t = \nu U_{yy}$), for which the solution is a thickening error function. While this profile resembles the Blasius profile (both having an inflection point at the wall), its stability characteristics are quite different. The critical Reynolds number based on the displacement thickness δ^* and the free-stream velocity U_∞ is about 2000, instead of 520. This would make comparisons with experiments impossible. This is why it was decided to add a small correction to (1) so that the laminar solution has a Blasius profile.

In addition, in the spatially developing boundary layer the TS wave amplitude and the thickness of the boundary layer grow simultaneously, on the same long, "viscous" length scale $U_\infty \delta^{*2} / \nu$. A given wave becomes unstable and starts growing when the flow crosses "Branch I" on the stability diagram (Schlichting 1979). It becomes stable again and starts decaying when the flow crosses "Branch II." If the mean flow did not evolve, the wave would experience steady exponential growth or decay. This difference is important, and it was decided that the modified form of (1) should allow the thickness to grow in time, while retaining a Blasius profile. The procedure is the following.

The solution of the Blasius equation provides the boundary-layer profile $U_B(y, X)$ as a function of y and of X , the distance from the leading edge. A correspondence between time and space is made by defining X as a function of t . A linear function was chosen

$$X = X_0 + ct. \quad (2)$$

The celerity c is chosen to match the growth rate of the boundary-layer thickness and the growth rate of the TS wave. The group velocity, c_g , is known to relate the temporal growth rate of spatially periodic TS waves and the spatial growth rate of time-periodic waves, if the growth rates are small and the mean flow is treated as parallel (Gaster 1962). Thus, c should be taken equal to c_g . The group velocity is not quite constant, because the boundary layer thickens, but this effect is weak. In the range of Reynolds numbers considered here, the group velocity is between about $0.38U_\infty$ and $0.42U_\infty$. A constant value $c = 0.4U_\infty$ will be used.

Introducing (2) into the function $U_B(y, X)$ defines the “desired” mean velocity profile $U_B(y, t)$. Equation (1) is modified by the addition of two terms,

$$\frac{\partial U}{\partial t} - \frac{\partial \tau}{\partial y} = \nu \frac{\partial^2 U}{\partial y^2} + \underbrace{\frac{\partial U_B}{\partial t} - \nu \frac{\partial^2 U_B}{\partial y^2}}. \quad (3)$$

If, in addition, the initial profile is

$$U(y, 0) = U_B(y, 0) \quad (4)$$

the solution $U(y, t)$ of (3,4) will satisfy

$$U(y, t) = U_B(y, t) \quad (5)$$

as long as τ is negligible. This applies to the laminar flow, and to the transitioning flow until the disturbances reach a nonlinear level.

This procedure of solving the mean momentum equation (3), albeit with an artificial term added, is preferable to the cruder procedure of just imposing (5) for all times, because it allows the disturbances to deform the mean velocity profile and extract energy from it. Thus the beginning of the nonlinear stage is clearly indicated (in practice, one can monitor the shape factor of the mean profile). The correction term in (3) acts only on the mean flow, and has no direct effect on the fluctuations. Of course, when the velocity profile loses its Blasius shape, the correction defined by (3) becomes inadequate. However, transitional breakdown occurs on the fast, convective time scale δ^*/U_∞ and the correction term, which acts on the slow, viscous time scale δ^{*2}/ν , has little effect. This fact was recognized by Wray & Hussaini (1984); they did not apply any correction, but started their simulation shortly before breakdown, so that the mean profile remained close to a Blasius profile until breakdown occurred. In the present study the boundary layer is followed for a much longer time in the linear stage, hence the need for a correction.

The system of modified equations has now been defined, and is solved by the numerical method that was described in Part 1. This method is spectral in space, with infinite-order accuracy, and uses second-order accurate finite differences in time. The initial TS amplitude is varied to obtain different types of breakdown. The overall amplitude of the random disturbances is also varied, as is the sequence of computer-generated random numbers. The amplitude of the random three-dimensional disturbances is statistically the same for all wave vectors in the horizontal plane (white noise). The disturbances also extend all across the domain in the y direction; several types of random y -dependence were tried without causing significant differences in the results. Thus the (arbitrary) disturbances are as unbiased as possible. Introducing selected three-dimensional disturbances is of course possible, but the resulting proliferation of additional parameters with unknown practical significance was thought to be undesirable.

3. Results

3.1. Physical and numerical parameters

The spatial and temporal accuracy of the method, when applied to a single TS wave, was tested in Part 1. These tests showed very good accuracy with the resolution that will be used throughout, namely 27 Jacobi polynomials and a value of about $3\delta^*/U_\infty$ for the time step. The amplitude ratio of the wave, from Branch I to Branch II, is also of interest and depends directly on the value of c . With $c = 0.4U_\infty$ the ratio is about 17 for the TS wave that will be considered below, which is the right magnitude. In the experiments of Saric *et al.* (1984) the ratio was about 25, and part of the growth was an artifact due to the smoke wire disturbing the mean flow.

The three-dimensional results will now be described. In a spatially developing boundary layer the frequency f of the TS wave is independent of X . In a time-developing boundary layer it is the streamwise wave number α that is independent of t . The nondimensional frequency F and the nondimensional wave number a , defined by

$$F \equiv 10^6 \frac{2\pi f\nu}{U_\infty^2} \quad \text{and} \quad a \equiv 10^3 \frac{\alpha\nu}{U_\infty}, \quad (6)$$

are related by

$$F = 10^3 a \frac{c_\phi}{U_\infty}, \quad (7)$$

where c_ϕ is the phase velocity of the wave. The quantity c_ϕ/U_∞ varies slightly in the neighborhood of 0.36 as the thickness grows, so that F varies by a few percent in the simulation. With the wave number a set to 0.21, F is close to 76, the value chosen by Saric *et al.* (1984). The Reynolds number $\sqrt{U_\infty X}/\nu$ at Branch II, for $a = 0.21$, is about 920.

In the x direction the numerical period is twice the TS wave period; the first subharmonic, with $a = 0.105$, is included. The period is about 40 times the displacement thickness at Branch II. There are 16 points in real space, and 5 nonzero wave numbers. In the z direction the lowest wave number is $b = 0.035$; the period is about 120 displacement thicknesses. This large period is chosen to allow a fine description of the spectrum in the z direction. In most cases, there are several z wave numbers within the bulge in the spectrum. Depending on the cases, there are 48 or 96 points in the z direction. The two-dimensional spectra that will be presented show how, in high-amplitude cases, higher spanwise wave numbers develop significant energy. This is why 96 points are used for these cases, while 48 are sufficient at low amplitudes. The same plots show that the resolution in the x direction is sufficiently fine.

With these values, the Reynolds number based on the grid spacing in the x or z direction is several thousand; the grid can be quite coarse because the viscosity plays a very small role in these directions. This is acceptable as long as the flow is smooth, but when breakdown occurs the spectrum fills up very rapidly and the simulation is no longer reliable. Simulations deeper into the breakdown phase will be possible only with much finer resolution and presumably with a smaller domain (Wray & Hussaini 1984).

The most important parameter is the root-mean-square (rms) amplitude A_{max} of the TS wave, measured at its peak. This peak corresponds to Branch II, unless nonlinear effects are present. If A_{max} is below about 0.3%, three-dimensional breakdown does not occur while the TS wave is the dominant disturbance (breakdown occurs much later, with a different mechanism). Between 0.3% and about 3%, subharmonic, C- or H-type breakdown

occurs, with increasing spanwise wave number. Above 3% the energy of the fundamental or K-type mode becomes comparable to the energy of the subharmonic mode, but a clear-cut K-type breakdown is never observed. In the experiments, the threshold amplitudes were lower: about 0.25% for subharmonic breakdown, and 1% for the fundamental type. These discrepancies were already observed by Spalart (1984) and will be discussed further.

3.2. Visualizations

Visualizations of the flow using passive particles will be shown first, and can be compared with the experimental visualizations using smoke (Saric *et al.* 1984). The motion of particles is computed using linear interpolation in space and the Runge-Kutta third-order scheme in time (see Part 1). Figure 1a shows the initial position of the particles. The coordinates are nondimensionalized by U_∞ and $10^3\nu$. The nondimensional displacement thickness is between 1.25 and 2. Six spanwise lines of 144 particles each are released at regular intervals in x . The height of release is adjusted so that the particles are near the critical layer when breakdown occurs. This is important; by keeping the particles in phase with the flow structures one greatly enhances the correspondence between the particle-line pattern and these flow structures. The particles cannot be *exactly* in the critical layer, if only because this layer moves up as the boundary layer thickens.

Figure 1b shows the particles after some time, but before three-dimensional effects are felt. The particles clustered into two bundles, revealing the two TS waves contained in the domain. Since the observation of these bundles as they subsequently deform is a major tool in both experimental and numerical studies, it is important to know which part of the wave is marked by the bundles. In particular, do they follow a "vortex?" Figures 1c and 1d are plots in a vertical x, y plane in the same situation as figure 1b (under the effect of the two-dimensional wave, but before breakdown) and at two different times. The y direction is magnified. The positions of the particles and vorticity contours are super-imposed. Figures 1b, 1c, and 1d are typical of the behavior at other times. The particles tend to gather in regions of higher-than-average vorticity, which are indicated by the upward bending of the vorticity contours.

This gathering is statistical rather than systematic. If a large number of particles is released, they form a cloud which is densest in the high-vorticity region (see figure 1e). Figure 1e corresponds most closely to the experimental situation, in which smoke is continuously emitted by the smoke wire and forms one cloud per TS wave period. In a reference frame moving with the phase velocity of the wave, the trajectories in the vicinity of the critical layer are shallow orbits. As a result, the particles that are caught in these orbits form a cloud that follows the wave. What figure 1e shows is that the center of the orbits roughly coincides with the "vortex" carried by the TS wave, which was not obvious a priori.

Figure 1f shows the particles at the time of breakdown, with $A_{max} = 1\%$, revealing a staggered pattern. The spanwise wave number b is 0.14, in very good agreement with the value of Saric *et al.* (1984). Figure 1g is at $A_{max} = 1.5\%$: the pattern is still staggered but is less regular, and the structures are narrower; b is about 0.2. This value agrees with the value measured by Saric *et al.* for an H-type breakdown, even though the value of A_{max} was different (0.4 %). The appearance of figures 1f and 1g is very similar to the experimental visualizations. Figure 1h is at $A_{max} = 4.8\%$; the breakdown pattern is irregular; it is no longer staggered, but is not convincingly aligned either. A breakdown pattern with well-aligned Λ vortices was never observed for any wave amplitude and time of visualization. One should note that in the experimental pictures, the breakdown that

is interpreted as a K-type looks much more irregular than the C- and H-type breakdowns (see figures 1 through 8 in Saric *et al.* (1984)). One may also ask whether the unsteadiness which Klebanoff *et al.* (1962) suppressed by adding strips of tape to the plate was due to the wavering of a well-defined K-type pattern, or to the kind of irregularity seen in figure 1h.

3.3. Quantitative results

Figure 2 shows histories of the shape factor H of the boundary layer, the amplitude of the TS wave, and the rms of the three-dimensional fundamental components (oblique waves with the same streamwise wave number as the TS wave) and subharmonic components (wave number half that of the of TS wave). The shape factor is plotted to signal when the mean velocity profile starts to depart from the Blasius shape. When breakdown occurs, H shows a clear tendency to decrease from its laminar value of 2.6 toward the turbulent value, about 1.5.

In figure 2a, $A_{max} = 0.1\%$. This amplitude is too low for breakdown to occur while the TS wave is the primary disturbance. However, there is a period of growth of the subharmonic mode. Thus, breakdown would occur if the initial background noise were sufficiently high. The TS wave decays beyond Branch II, following linear theory. The fundamental-mode energy also decays steadily. In figure 2b, with $A_{max} = 1\%$, the subharmonic component becomes unstable, grows rapidly, and causes breakdown. A similar behavior is observed in figure 2c, with $A_{max} = 1.5\%$. In both cases, a sudden reversal of the decay of the TS wave is the first indication of nonlinearity. The TS wave is presumably receiving energy from the subharmonic components through the nonlinear term (the subharmonic amplitude has reached several percent). Finally, in figure 2d with $A_{max} = 4.8\%$, the fundamental-mode energy becomes significant. However it does not dominate the subharmonic energy. In this last case, the occurrence of breakdown is revealed by the shape factor and the TS wave amplitude simultaneously.

Figure 3 presents a more detailed description of the fluctuations, using two-dimensional spectra at selected times. The u component in a horizontal plane was Fourier-transformed in the x and z directions and the energies of the four wave vectors ($+ - a, + - b$) were added. The plane chosen is near the critical layer; the fluctuations are known to be quite strong in that layer. A logarithmic scale is used for the energy, and values lower than 10^{-12} are not plotted to distinguish between the random noise and the relevant, energetic wave vectors. Except for the mean flow and the TS wave, any component that exceeds 10^{-12} in energy has experienced a significant amplification since the beginning of the simulation. In the far corner of the figure is the mean component. Along the far left boundary are the two-dimensional components (the TS wave and its higher harmonic).

In figure 3a with $A_{max} = 0.1\%$ a three-dimensional wave, while not strong enough to cause breakdown, has been amplified and is clearly defined. The spectrum shows a sharp peak with spanwise wave number $b = 0.14$. In figure 3b with $A_{max} = 1\%$ the subharmonic component dominates, with a sharp peak at $b = 0.14$ (as indicated by the visualizations) and a swelling at higher values ($b \approx 0.25$). At a higher amplitude, 1.5% , the spectrum is much broader (figure 3c). There is still a peak at $b = 0.14$, but there is also a broad band of energetic wave numbers from $b \approx 0.1$ to $b \approx 0.7$. These results are in agreement with Herbert (1984). At the highest amplitude, $A_{max} = 4.8\%$, both the subharmonic and the fundamental mode have acquired energy and have a broad spectrum (figure 3d), which results in the disordered pattern of figure 1h. Again the results agree with Herbert's 1985 results, in that the subharmonic mode is still strong even at high TS wave amplitudes.

To make a quantitative comparison between Herbert's results and those obtained here, the growth rates computed by Herbert (1985) at $F = 58.8$ were computed with the present method. The boundary-layer thickness and the TS wave amplitude were artificially kept constant to simulate Herbert's conditions (quasi-steady assumption). The flow was allowed to evolve until the growth rates of the three-dimensional disturbances became steady, indicating that the most unstable components had been selected. The comparison is shown in figure 4, using Herbert's units, and is satisfactory.

The determination of the dominant spanwise wave number allows one to test Craik's hypothesis (Craik 1971). For Craik's mechanism to explain the growth of the oblique waves, their phase velocity and that of the two-dimensional wave must be close. In figure 5a the band of energetic spanwise wave numbers is plotted as a function of A_{max} . The wave numbers were deduced from the visualizations; they increase with A_{max} . In figure 5b the phase velocity (in the x direction) of the two-dimensional and of the dominant oblique waves are plotted. When A_{max} exceeds about 1 %, most of the energy is carried by wave numbers that do not satisfy Craik's criterion. These results support Herbert's (1984) contention that Craik's mechanism is active at low TS-wave amplitudes, but cannot account for all of the three-dimensional activity at high amplitudes. Herbert's model describes ribbon-induced transition better; Craik's may be more relevant in natural transition.

3.4. Sensitivity to some of the parameters

The disturbance created by a vibrating ribbon in an experimental boundary layer is not a pure TS wave, and it takes some distance for the other components to decay. In addition the ribbon and the smoke wire disturb the mean velocity profile (Saric *et al.* 1984). This is why they must be far enough upstream of the region where measurements are taken. This distance is the "fetch". In the simulations a pure TS wave can be input, and the mean profile is not disturbed at all. Thus the need for a long fetch is not as strong. However, the three-dimensional disturbances are random, and no attempt is made to control their shape. Thus there is a period during which the various components get sorted, so that only the unstable, or weakly stable, ones survive. This is revealed by figure 2: the shape factor remains at 2.6 and the amplitude of the TS wave grows smoothly from the initial station, but the three-dimensional energy has rapid variations at the very beginning of the simulation. However, figure 2 also shows that this "unphysical" regime is over long before breakdown occurs. This means that the fetch is long enough. The smoothness of the spectra, presented in figure 3, confirms this impression. Simulations were conducted with longer fetches (starting near Branch I) and the results were not significantly different.

The type of the breakdown mostly depends on the peak amplitude A_{max} of the TS wave. However, it also depends on the initial amplitude A_{3D} of the three-dimensional random disturbances, or "noise level," especially if A_{max} is near a threshold. Simulations were conducted with $A_{max} = 0.5\%$ and two values of A_{3D} . The rms of the three-dimensional components, after the initial transient, was about 2×10^{-5} and 2×10^{-6} , respectively. The results are shown in figure 6. Breakdown occurs only with the higher value of A_{3D} . This case, $A_{max} = 0.5\%$, was classified as transitional because the three-dimensional component was amplified by three orders of magnitude. The $A_{max} = 0.1\%$ case was not, because the amplification was only one order of magnitude (figure 2a). This illustrates the impossibility of sharply defining threshold values in terms of A_{max} alone. The difference between the experimental and the numerical estimates of the lowest value of A_{max} that will result in breakdown (0.25% and 0.3%, respectively) is not serious.

The effect of the random numbers used for the initial disturbance was also studied. Figure 7 shows the energy histories for two simulations which had the same disturbance amplitude, but different random-number sequences. The three-dimensional energy is at slightly different levels, but the growth pattern is the same. Because of the different level of energy, breakdown occurs at slightly different stations. The scatter in the breakdown Reynolds number is of the order of 10, and is quite small compared with the scale of the early stages of transition, which is hundreds of Reynolds number units. This result suggests that the use of random numbers for the initial disturbance is appropriate.

Finally, the effect of the computational periods Λ_x and Λ_z which, ideally, would be infinite, was studied by doubling them. Figure 8 is a visualization of the flow with Λ_z doubled and $A_{max} = 1.5\%$. The breakdown pattern is still somewhat irregular, but is obviously an H-type. There are no major differences between this figure and figure 1g. This indicates that the original value of Λ_z is sufficient. The period Λ_x was then doubled, to investigate the possibility of another period doubling in the x direction, similar to the difference between K- and H-type breakdown. Figure 9a is a visualization of the flow. The difference between the two halves of the domain, in the x direction, is small but noticeable. This suggests that enough randomness was present to trigger an instability, if such an instability exists. The spectrum, shown in figure 9b, reveals significant energy in the "sub-subharmonic" region. However, the first subharmonic mode still dominates. The results in figures 8 and 9 suggest the possibility of generating incipient turbulent spots by using large enough periods both in the x and z directions.

3.5. Discussion

The results presented in this chapter are in good agreement with Herbert's analysis, and their sensitivity to the arbitrary parameters that had to be prescribed was shown to be very moderate. The agreement with Saric *et al.*'s experimental results is good for the lower values of A_{max} . On the other hand, the computed threshold between the C-type breakdown (wide structures in the z direction) and the H-type (narrower structures) is over 1%, when the experimental value is about 0.35%. In addition, a pure K-type breakdown is never predicted even at high amplitudes (one could argue that Saric *et al.*'s visualizations, especially their figure 8, show some of the features of a mixed-type breakdown). The trend is for the numerical results to match the experimental results at lower amplitudes (see the spanwise wave number of the H-type breakdown). Both sets of results show C-type breakdown occurring beyond Branch II, H-type breakdown near Branch II, and K- or mixed-type breakdown upstream of Branch II, the computed breakdown being slightly farther downstream (compare our figure 2 and Saric *et al.*'s figure 5). The agreement could probably be improved further by raising the noise level in the simulations.

The behavior of the flow for A_{max} near the C- to H-type threshold is illustrated by the spectra in figures 3a and 3b. They show that the C-mode ($b = 0.14$) grows first, when the TS wave amplitude is low. Further downstream, if A_{max} is high enough, the H-mode (broad-band) grows. It may or may not "catch up" with the C-mode before breakdown. Figures 1f and 3b show that with $A_{max} = 1.0\%$ it did not catch up, resulting in a C-type breakdown. The competition between the two modes depends, to some extent, on the fetch and on the noise level. The same can be said of the competition between the H- and K-modes; figure 2d shows the K-mode starting from a lower level, but consistently having a slightly larger growth rate than the H-mode.

These considerations show that the disagreement between numerical and experimental results cannot be considered as final unless *all* the disturbances, including the ones that are classified as “noise,” are completely controlled. Herbert (1985) studied Klebanoff *et al.*'s 1962 experiment in detail. The experiment produced a K-type breakdown, but Herbert's theory predicts an H-type, since the computed subharmonic-mode growth rates are consistently higher than the fundamental-mode growth rates (figure 4). He concluded that in the experiment the fundamental mode was receiving more energy than the subharmonic mode because of nonuniformity of the mean flow in the z direction.

One should also keep in mind the sources of error in the theoretical and numerical studies. The “ideal situation” is a perfectly uniform, spatially developing boundary layer, with spatially developing disturbances. Like Herbert, we are treating a parallel mean flow and time-developing disturbances. The nonparallel character of the mean flow is known to affect the critical Reynolds number of linearized TS waves to some extent; its effect here is unknown. The periodic assumption loses some of its validity precisely at the beginning of the nonlinear stage, when the growth rates increase (the experimental visualizations show the three-dimensionality changing from unnoticeable to strong in about three wave lengths). Thus the question of which type dominates in the “ideal situation” should be considered an open one. A definitive answer can only come from refined experiments, or from simulations or theories in which the parallel-mean and periodicity assumptions have been discarded.

4. Conclusions

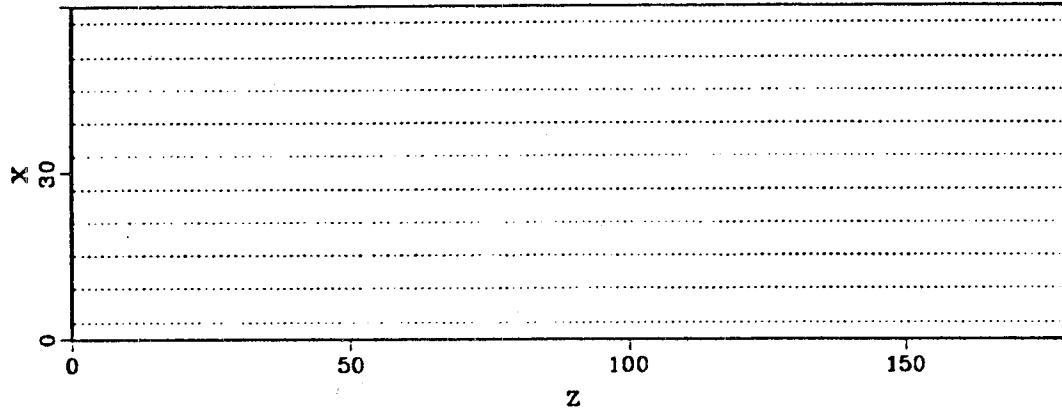
The early three-dimensional stages of ribbon-induced transition in a Blasius boundary layer were simulated numerically. The mean flow was treated as parallel and the disturbances as spatially periodic and time developing. The concurrent growth of the boundary-layer thickness, the two-dimensional wave amplitude, and the three-dimensional disturbance amplitude was reproduced. The numerical periods and the type of disturbances were chosen to influence the physical processes as little as possible. Tests were conducted to rule out a strong dependence on numerical parameters.

The results are in agreement with Craik's analysis for low TS-wave amplitude, and with Herbert's analysis for all amplitudes. The agreement with Saric *et al.*'s experiments is good at low amplitudes, but only fair at higher amplitudes. For a given amplitude, the numerical results tend to agree with experimental results corresponding to lower amplitudes. The disagreement is at least partly explained by differences in the three-dimensional excitation of the boundary layer, even though in both cases it had a random character. This illustrates again the extreme sensitivity of transitional phenomena in a Blasius flow. It suggests that further study of these fine effects should focus on devising the most credible procedure to input disturbances, and may be less useful than the study of pressure-gradient or cross-flow effects, which are much more powerful and are present in most flows of interest.

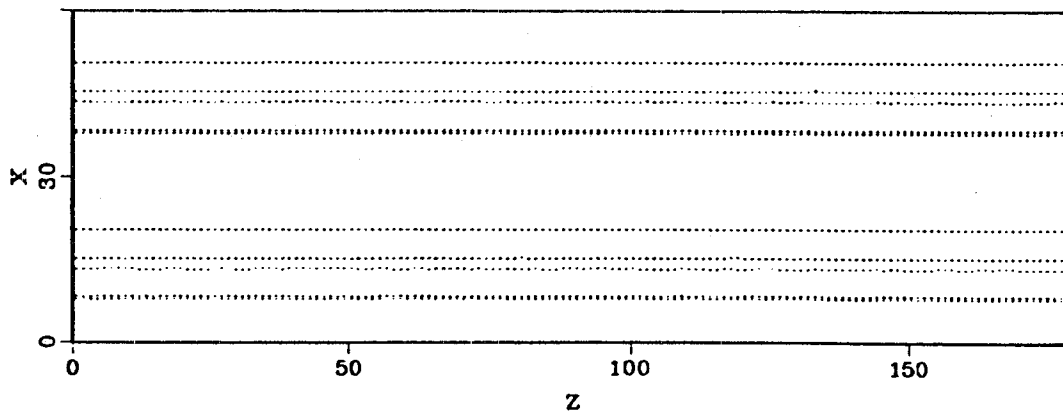
The authors thank Dr. A. Wray, from NASA Ames Research Center, and Profs. H. Reed and J. Ferziger from Stanford University for useful discussions. The second author was supported by the A.F.O.S.R. under grant 84-0083.

REFERENCES

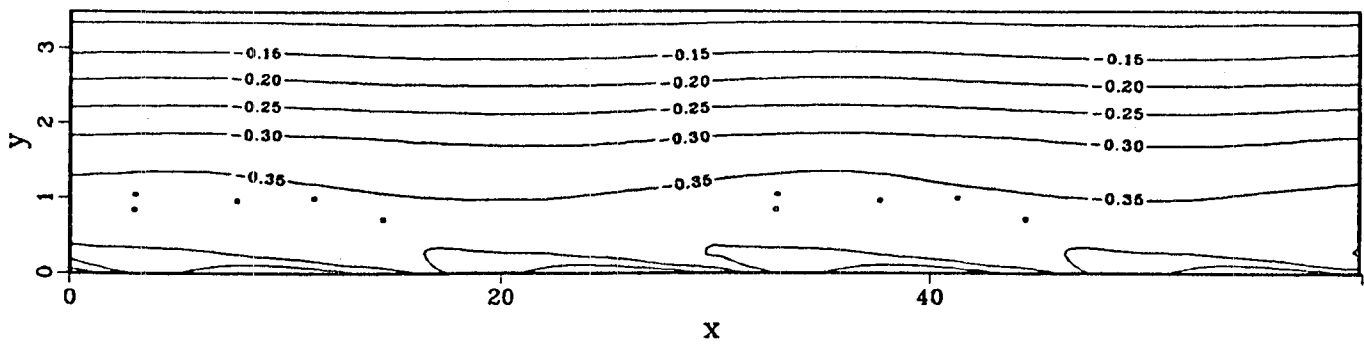
- Craik, A. D. D. 1971** Nonlinear resonant instability in boundary layers. *J. Fluid Mech.* **50**, 2, 393-413.
- Gaster, M. 1962** A note on the relationship between temporally increasing and spatially increasing disturbances in hydrodynamic stability. *J. Fluid Mech.* **14**, 222.
- Herbert, T. 1984** Analysis of the subharmonic route to transition. *AIAA-84-0009*.
- Herbert, T. 1985** Three-dimensional phenomena in the transitional flat-plate boundary layer. *AIAA-85-0489*.
- Kachanov, Y. S. & Levchenko, V. Y. 1984** The resonant interaction of disturbances at laminar-turbulent transition in a boundary layer. *J. Fluid Mech.* **138**, 209-247.
- Klebanoff, P. S. Tidstrom, K. D. & Sargent, L. M. 1962** The three-dimensional nature of boundary layer instability. *J. Fluid Mech.* **12**, 1-34.
- Kovaszny, L. S. G. Komoda, H. & Vasudeva, B. R. 1962** Detailed flow field in transition. *Proc. 1962 Heat transfer and Fluid Mechanics Institute* 1-26.
- Orszag, S. A. & Kells, L. C. 1980** Transition to turbulence in plane Poiseuille and plane Couette flow. *J. Fluid Mech.* **96**, 159-205.
- Saric, W. S. Kozlov, V. V. & Levchenko, V. Y. 1984** Forced and unforced subharmonic resonance in boundary-layer transition. *AIAA-84-0007*.
- Schlichting, H. 1979** Boundary layer theory. 7th ed. McGraw-Hill, New York.
- Spalart, P. R. 1984** Numerical Simulation of Boundary-Layer Transition. 9th Int. Conf. on Num. Meth. in Fluid Dyn., Paris, June 1984.
- Wray, A. & Hussaini, M. Y. 1984** Numerical experiments in boundary-layer stability. *Proc. Roy. Soc. London A* **392**, 373-389.



a) Initial position, top view.

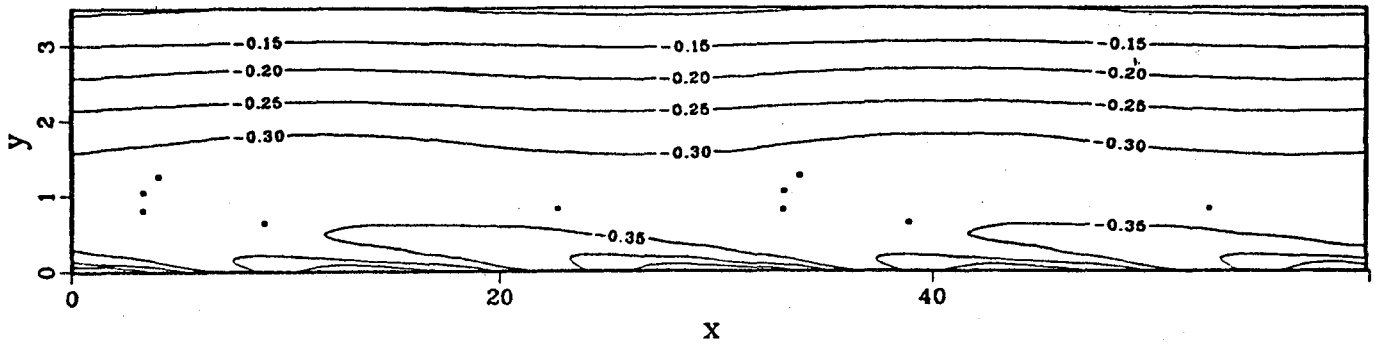


b) Before three-dimensional breakdown, top view.

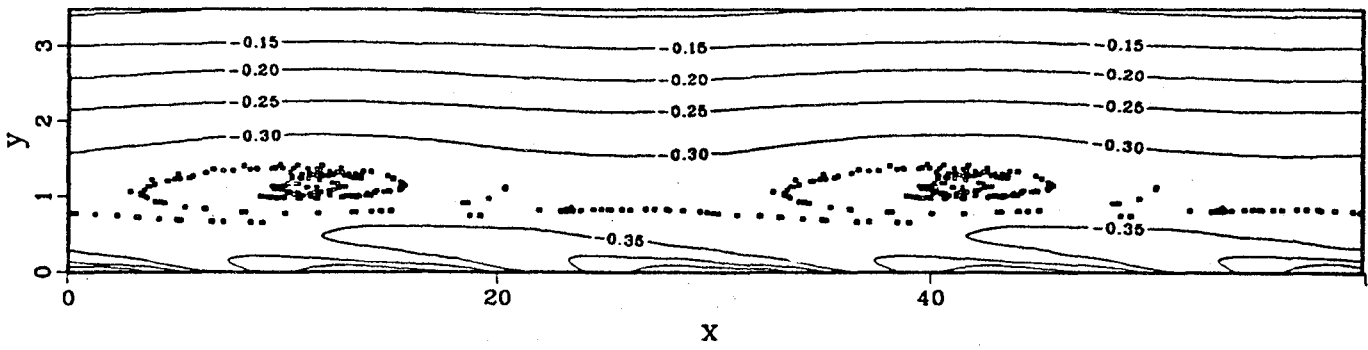


c) Before three-dimensional breakdown, side view.

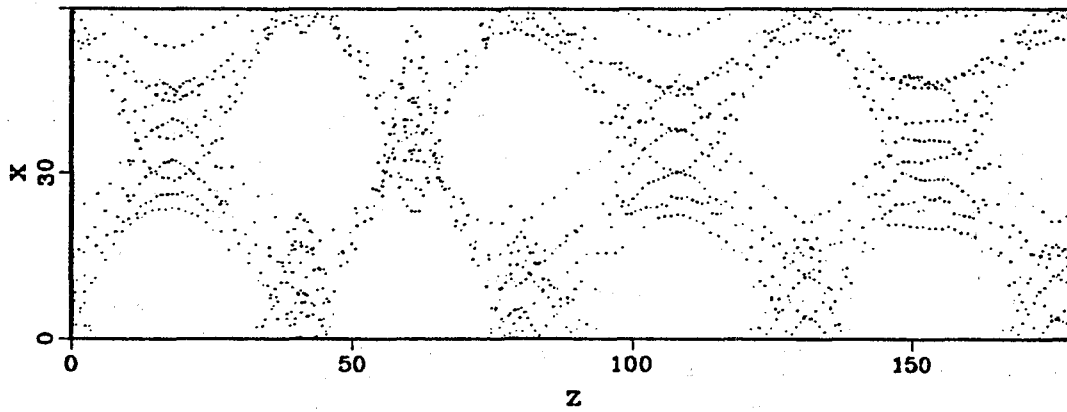
Figure 1. Flow visualization by passive particles. x direction streamwise, y normal, z spanwise. — vorticity contours.



d) Before three-dimensional breakdown, side view, later in time.

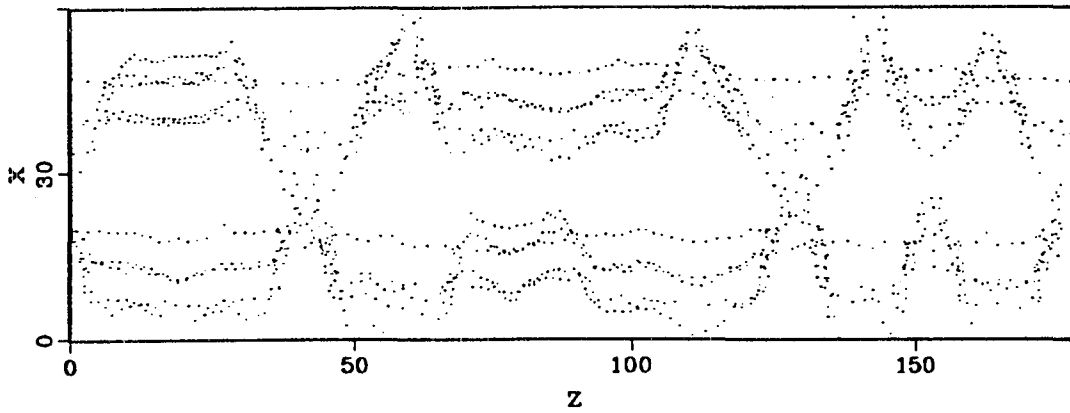


e) Before three-dimensional breakdown, with large number of particles.

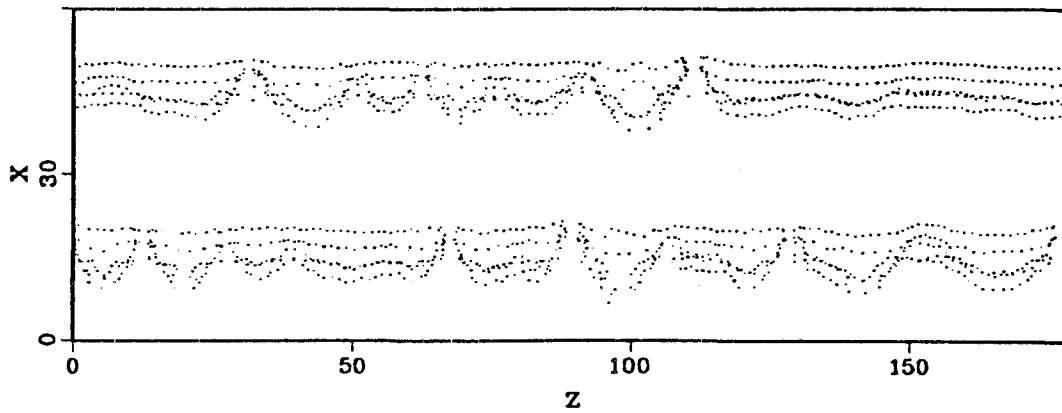


f) Beginning of breakdown, $A_{max} = 1\%$.

Figure 1, continued.

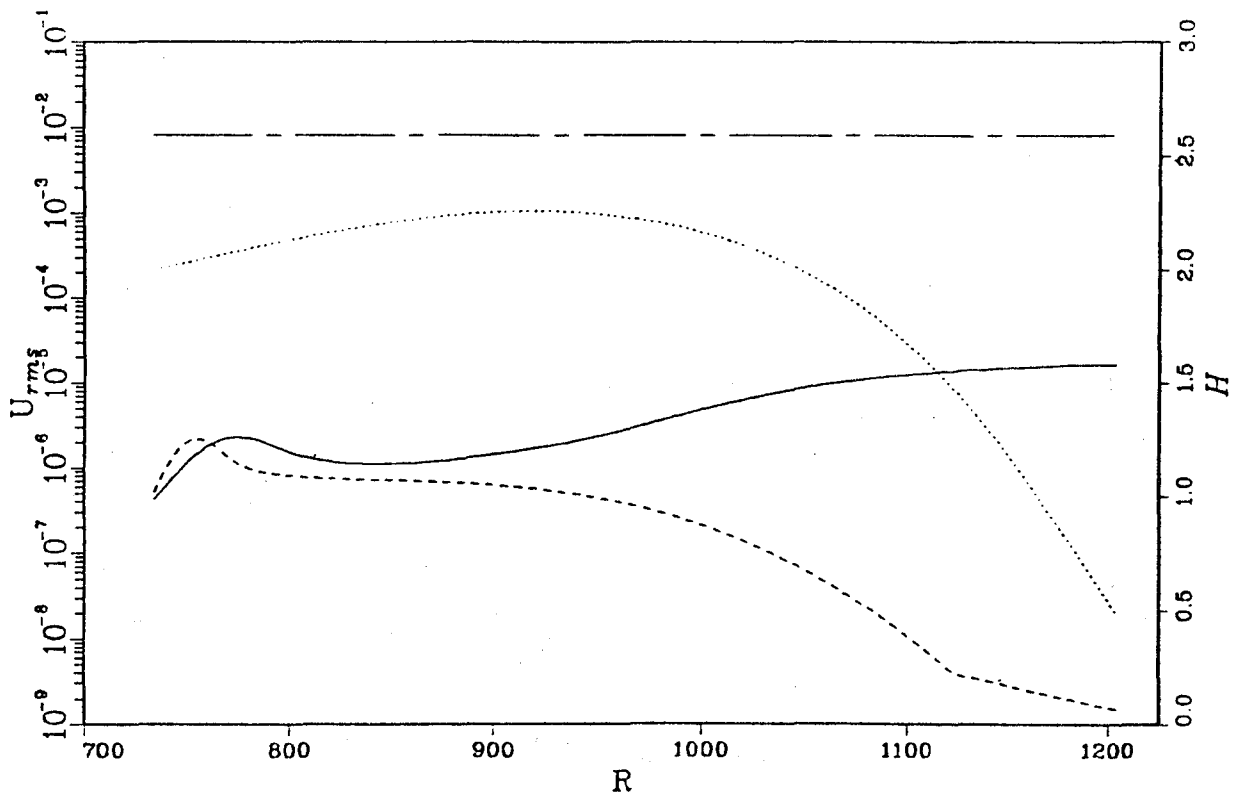


g) Beginning of breakdown, $A_{max} = 1.5\%$.

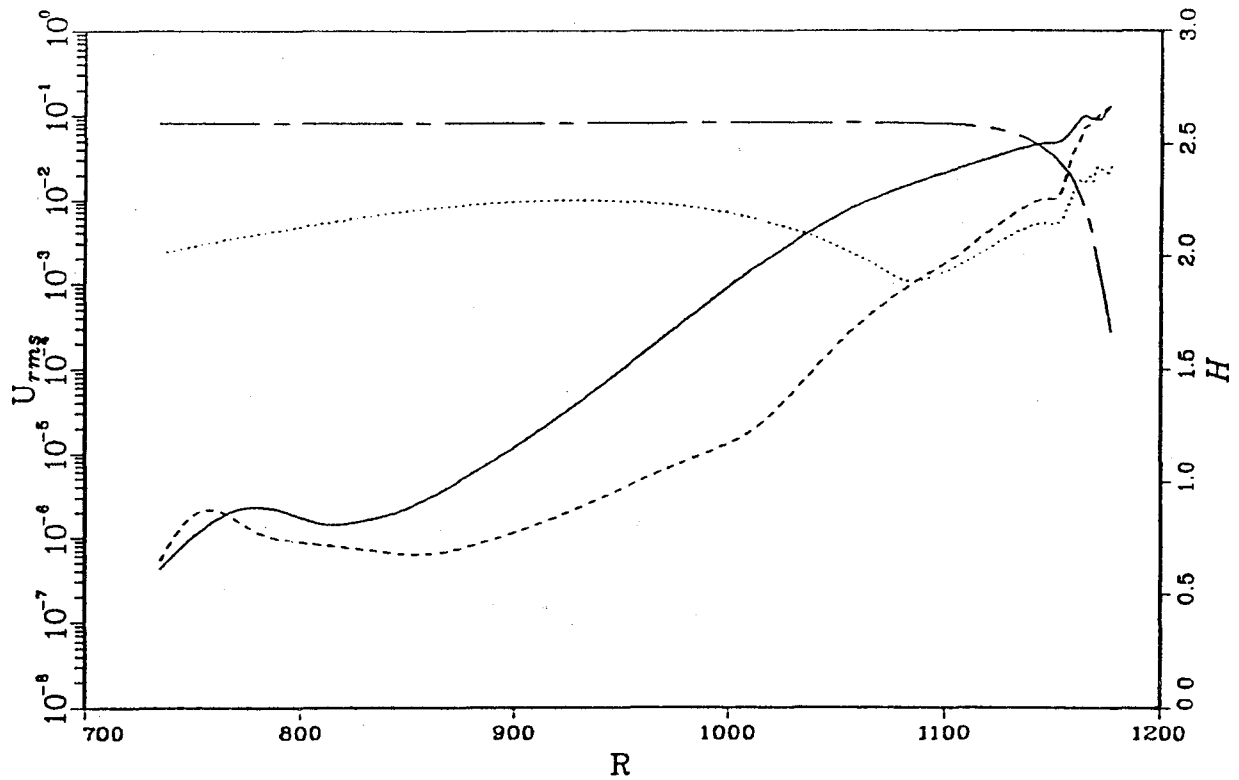


h) Beginning of breakdown, $A_{max} = 4.8\%$.

Figure 1, concluded.

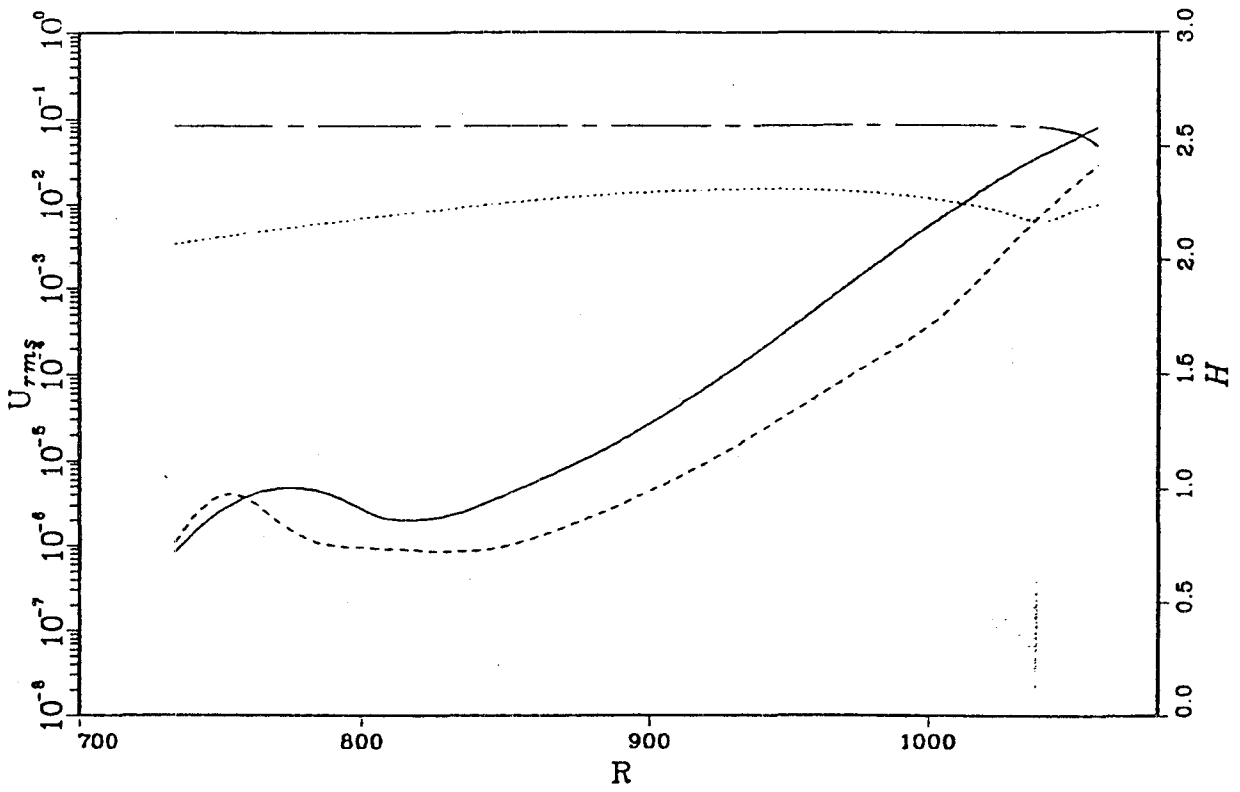


a) $A_{max} = 0.1\%$.

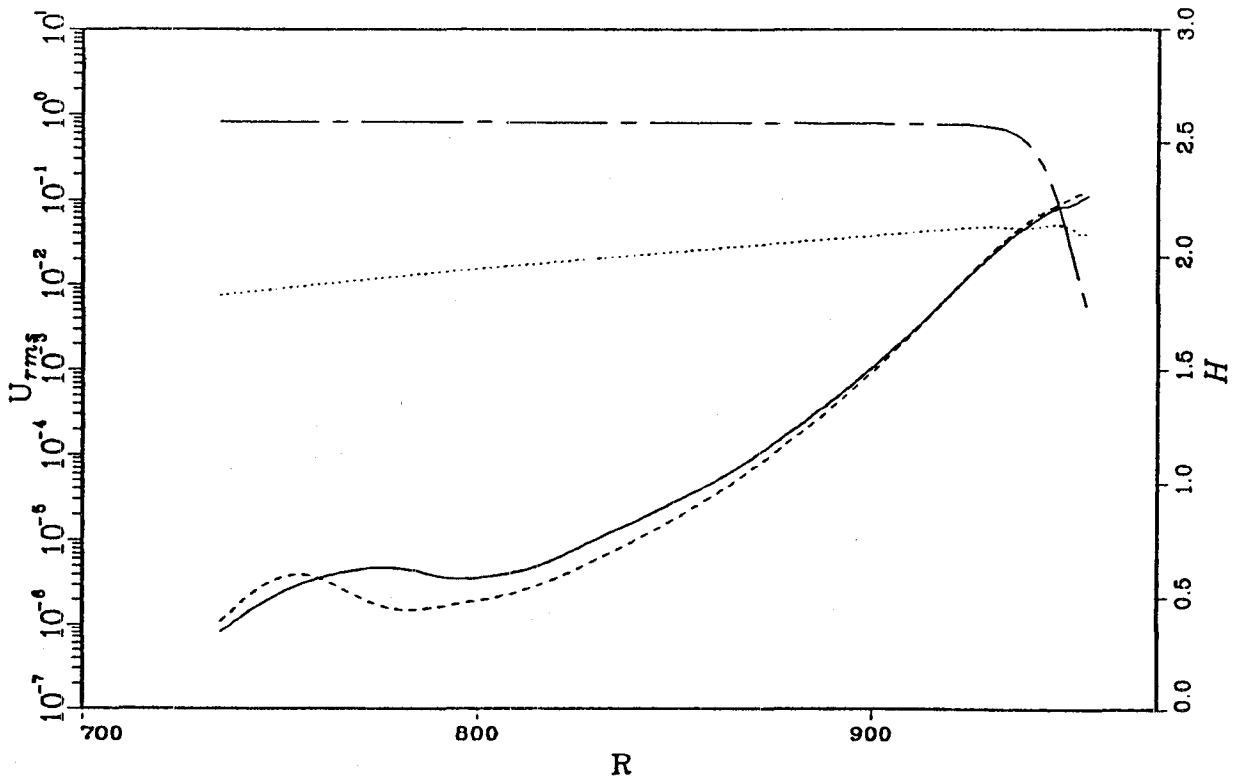


b) $A_{max} = 1.0\%$.

Figure 2. Time history. - - - shape factor H ; ... two-dimensional TS wave rms; — three-dimensional subharmonic mode rms; - - - three-dimensional fundamental mode rms.

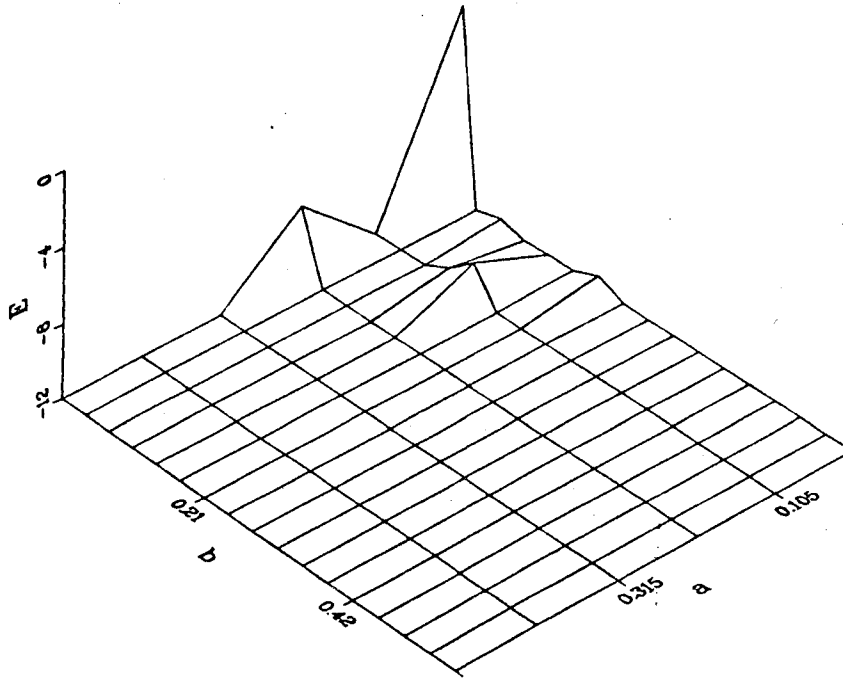


c) $A_{max} = 1.5\%$.

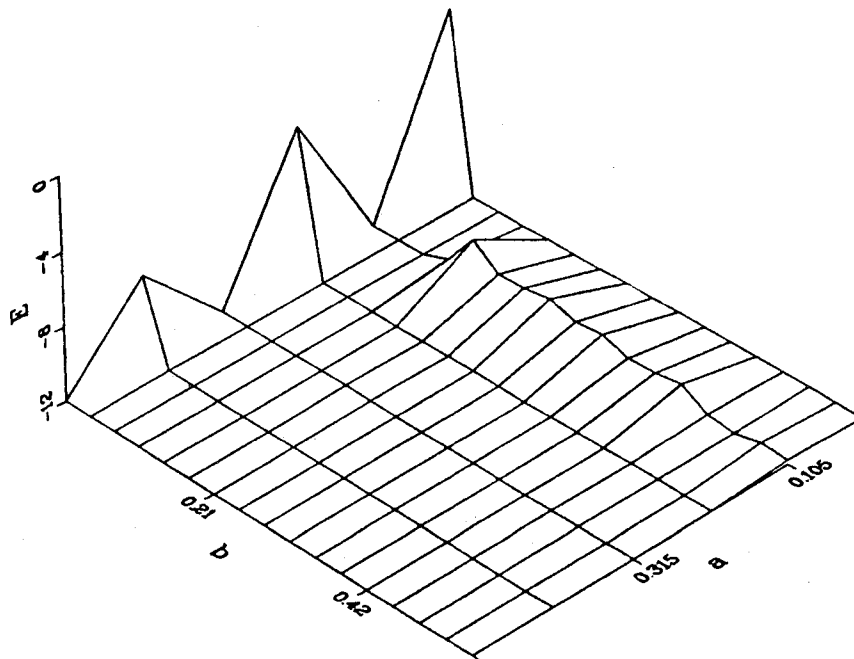


d) $A_{max} = 4.8\%$.

Figure 2, concluded.

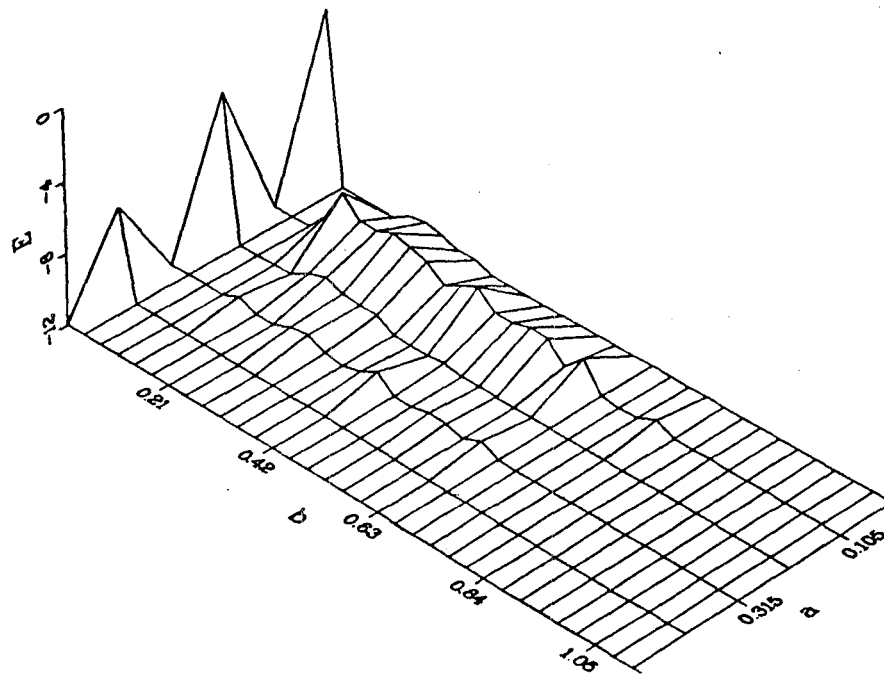


a) $A_{max} = 0.1\%$, $t = 1750$, no breakdown.

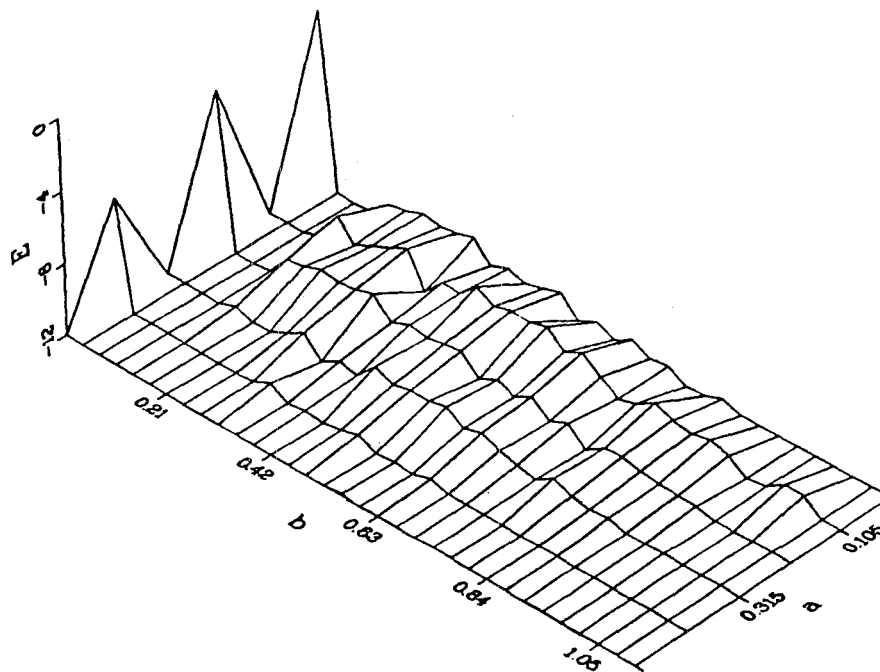


b) $A_{max} = 1.0\%$, $t = 770$, subharmonic breakdown.

Figure 3. Two-dimensional energy spectrum. a streamwise wave number, b spanwise. Energy scale logarithmic, base 10.



c) $A_{max} = 1.5\%$, $t = 760$, subharmonic breakdown.



d) $A_{max} = 4.8\%$, $t = 510$, mixed-type breakdown.

Figure 3, concluded.

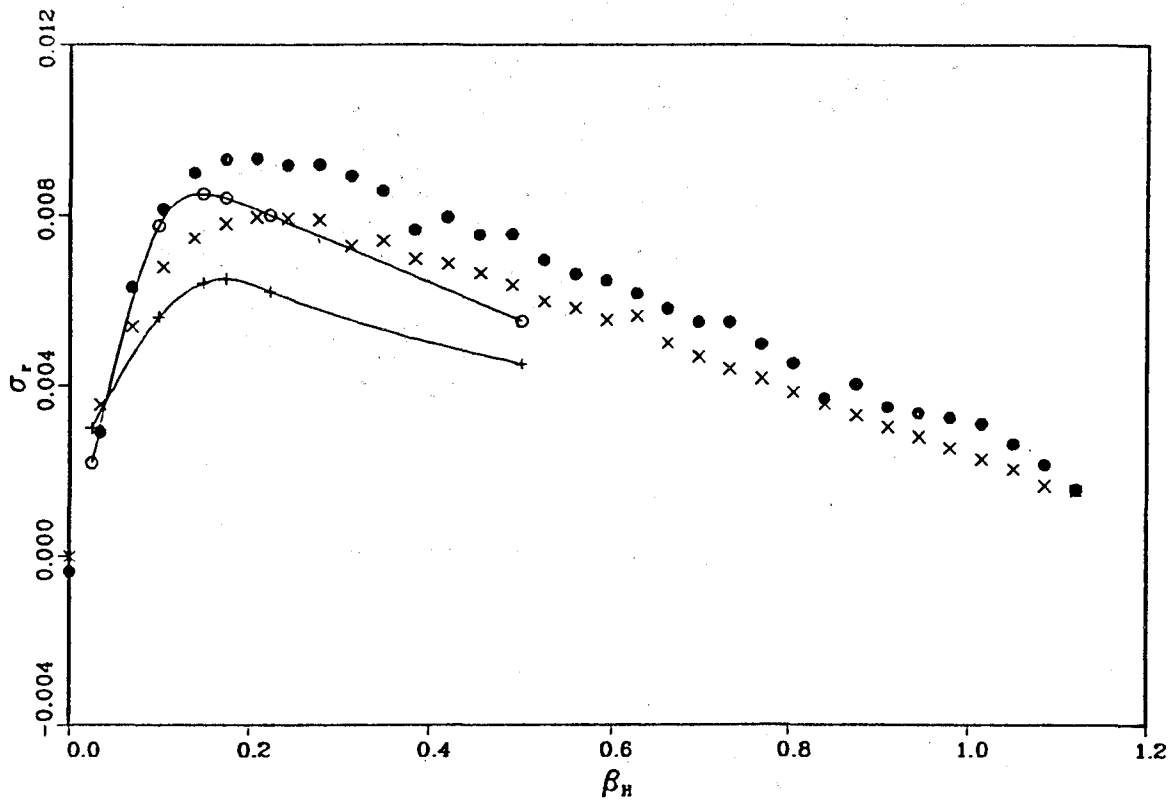


Figure 4. Growth rate of three-dimensional disturbances. Present results: ● subharmonic, × fundamental. Herbert: ○ subharmonic, + fundamental.

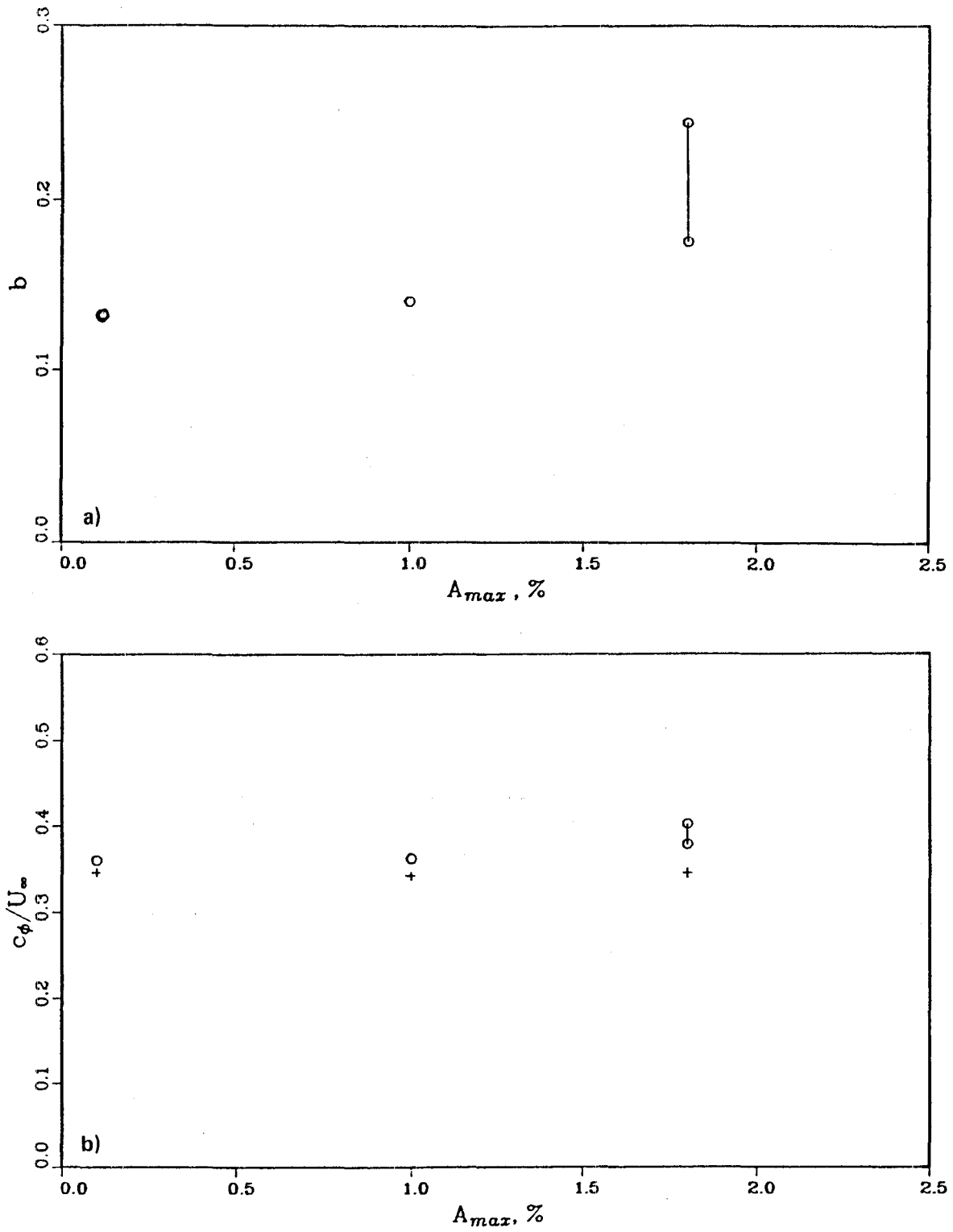


Figure 5. Characteristics of dominant subharmonic wave. a) Spanwise wave number; b) phase velocity. o three-dimensional wave, + two-dimensional wave.

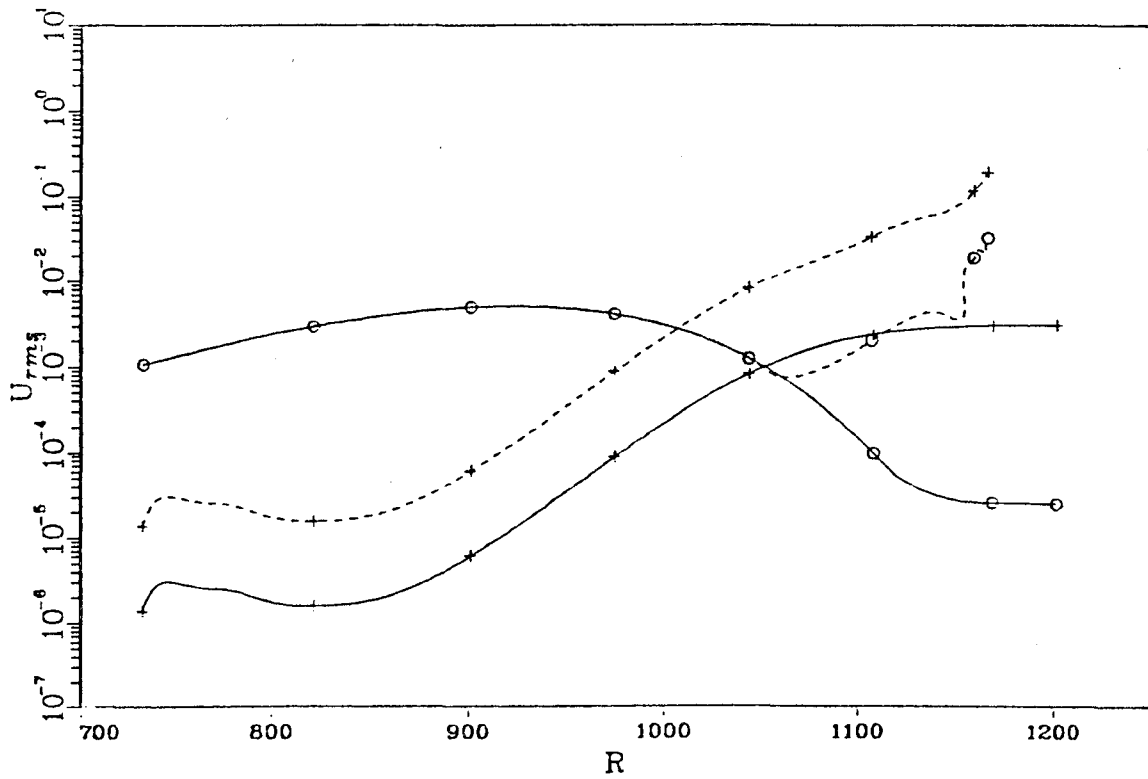


Figure 6. Effect of noise level on breakdown, $A_{max} = 0.5\%$. o two-dimensional wave, + three-dimensional wave. — low level, - - - high level.

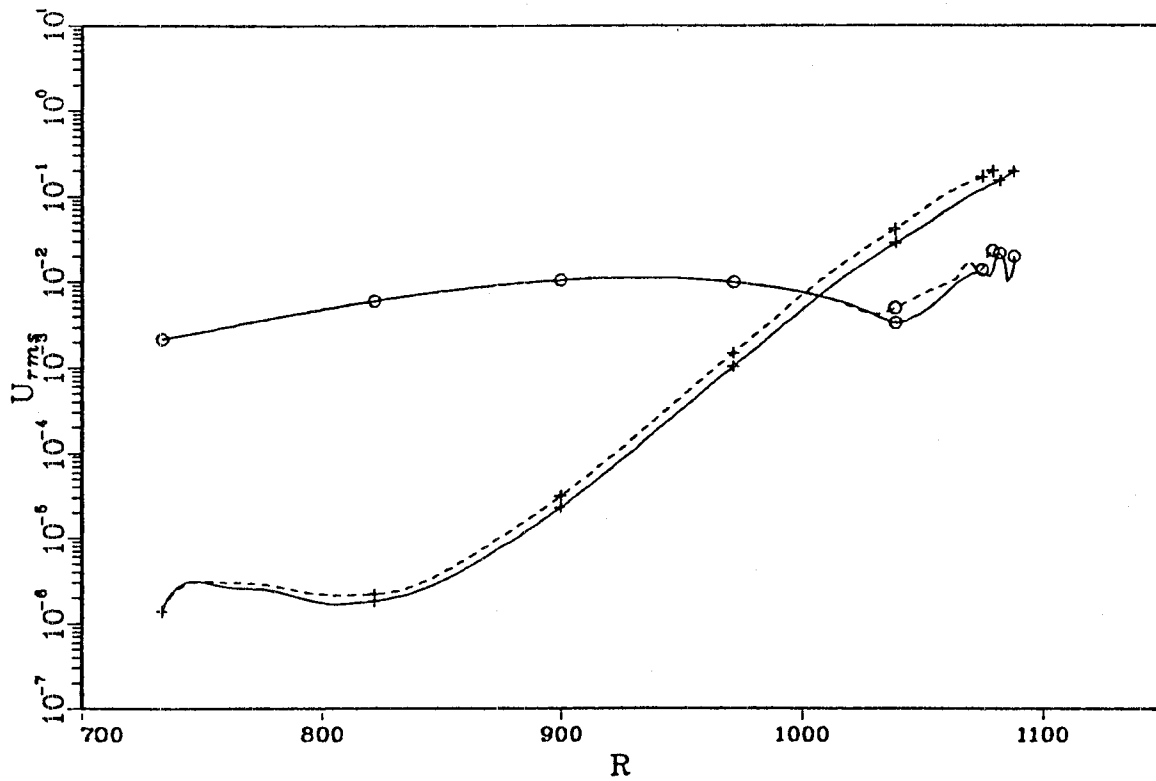


Figure 7. Effect of random number sequence on breakdown, $A_{max} = 1.5\%$. o two-dimensional wave, + three-dimensional wave. — first sequence, - - - second sequence.

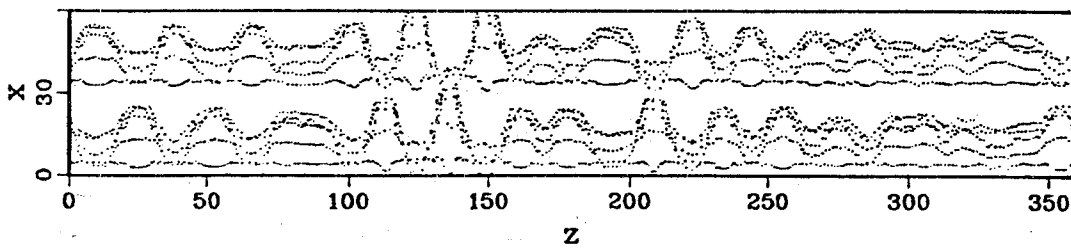
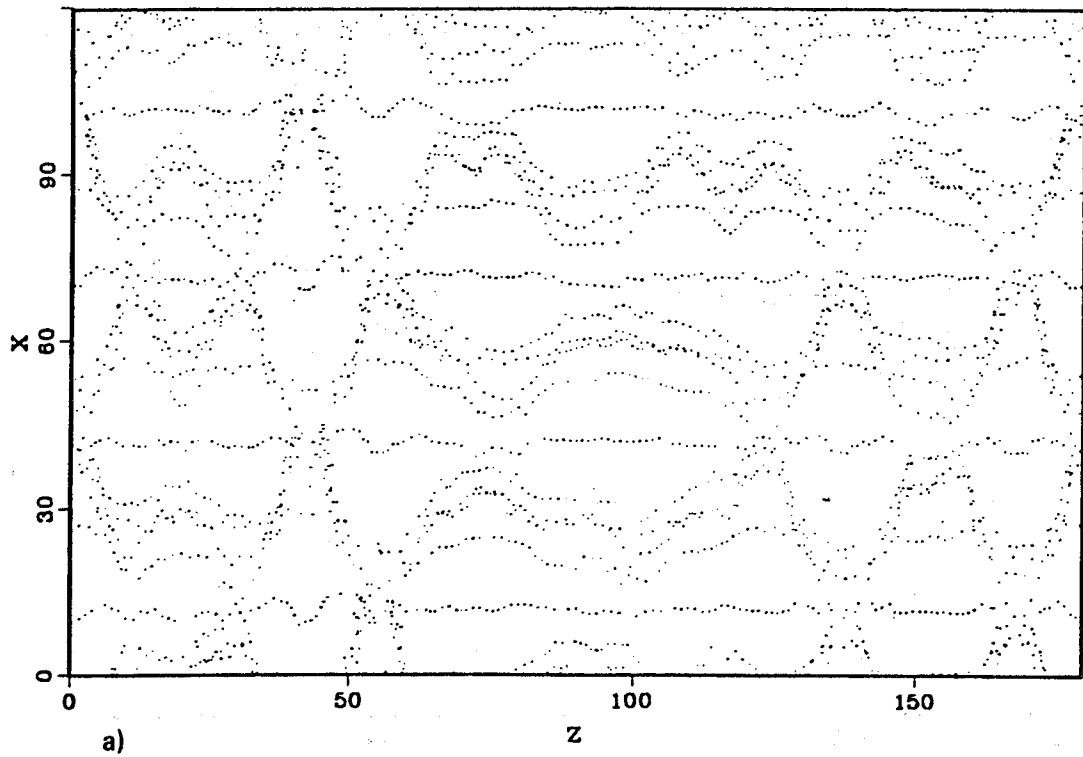
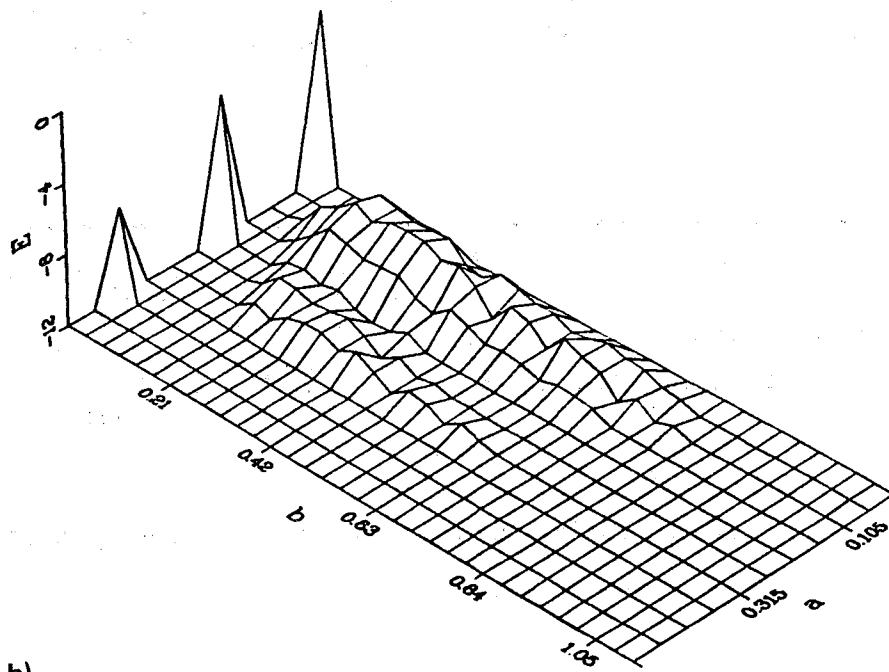


Figure 8. Simulation with increased Λ_z , $A_{max} = 1.5\%$. See figure 1g.



a)



b)

Figure 9. Simulation with increased Λ_x , $A_{max} = 1.5\%$. a) Passive particles, b) spectrum. See figures 1g and 3c.

1. Report No. NASA TM-88221	2. Government Accession No.	3. Recipient's Catalog No.	
4. Title and Subtitle NUMERICAL SIMULATION OF BOUNDARY LAYERS. PART 2. RIBBON-INDUCED TRANSITION IN BLASIUS FLOW		5. Report Date February 1986	6. Performing Organization Code RFT
		8. Performing Organization Report No. A-86072	10. Work Unit No.
7. Author(s) Philippe Spalart and Kyung-Soo Yang (Stanford University, Stanford, CA)		11. Contract or Grant No.	
9. Performing Organization Name and Address Ames Research Center Moffett Field, CA 94035		13. Type of Report and Period Covered	
		14. Sponsoring Agency Code 505-60	
12. Sponsoring Agency Name and Address National Aeronautics and Space Administration Washington, DC 20546		15. Supplementary Notes Point of contact: Philippe R. Spalart, Ames Research Center, MS 202A-1, Moffett Field, CA 94035 (415)694-6667 or FTS 464-6667	
16. Abstract The early three-dimensional stages of transition in Blasius boundary layers are studied by numerical solution of the Navier-Stokes equations. A finite-amplitude two-dimensional wave and random low-amplitude three-dimensional disturbances are introduced. Rapid amplification of the three-dimensional components is observed and leads to transition. For intermediate amplitudes of the two-dimensional wave the breakdown is of subharmonic type, and the dominant spanwise wave number increases with the amplitude. For high amplitudes the energy of the fundamental mode is comparable to the energy of the subharmonic mode, but never dominates it; the breakdown is of mixed type. Visualizations, energy histories, and spectra are presented. The sensitivity of the results to various physical and numerical parameters is studied. The agreement with experimental and theoretical results is discussed.			
17. Key Words (Suggested by Author(s)) Numerical simulation Boundary layers Transition Turbulence		18. Distribution Statement Unlimited Subject category: 34	
19. Security Classif. (of this report) Unclassified	20. Security Classif. (of this page) Unclassified	21. No. of Pages 26	22. Price* A03

End of Document